Propagation Without Wave Equation Toward an Urban Area Model

Giorgio Franceschetti, *Fellow, IEEE*, Stefano Marano, and Francesco Palmieri

***Abstract*— Propagation in random media is a topic of great interest, whose application fields include, among others, the so-called last mile problem as well as the modeling of dense urban area radio communication channels. In this paper, a simple scenario for this issue is considered, with an optical-ray propagation across a medium of disordered lossless scatterers. The propagation medium behaves like a percolating lattice and the goal is to characterize statistically the propagation depth in the medium as a function of the density q of scatterers and of θ—the ray incidence angle. To the best of our knowledge, this approach is totally new. The problem is mathematically formulated as a random walk and the solutions are based on the theory of the martingale random processes. The obtained (approximate) analytical formulas have been validated by means of numerical simulations, demonstrating the applicability of the proposed model for a wide range of the global parameters q and θ. We believe that our results may constitute a promising first step toward the solution of more complicated propagation models and a wide class of communication problems.**

***Index Terms*—Last mile problem, propagation in random media, urban area communications.**

I. Introduction

DURING the last few years the problem of setting efficient fast communication links in dense populated areas has attracted increasing interest. Use of radio waves as a convenient alternative to most traditional cable or fiber connections has been suggested [1]–[4]. This solution is usually referred to as *the last mile* approach, whereas a terminal area of limited extension is served by means of radio links, instead of wires. This area may be a limited section of a city, a few buildings, or even a single building. Models, algorithms and mathematical tools for prediction of the electromagnetic signal characteristics in this situation is becoming of critical importance.

The natural starting point to approach the problem analytically may appear to be the huge existing literature about propagation in random media. A good comprehensive reference book is [5]. In particular, in the *line-of-sight* situation the transmitters send a signal trough a random medium and the objective of the model is to characterize the statistical behavior of the received signal. Quite sophisticated statistical characterizations of such a scenario are available in the literature, but unfortunately, a little thought shows that all these results are not applicable to our problem. In fact, the scatterers are assumed to be either small compared to the (incident) wavelength λ [6], i.e.,

$$\frac{2\pi d}{\lambda} \ll 1 \tag{1}$$

(d is a typical dimension of the scatterers), or large, but *tenuous* [7],

$$\frac{2\pi d}{\lambda} \gg 1, \qquad \epsilon_r - 1 \ll 1 \tag{2}$$

with ϵ_r being the relative dielectric constant of the scatterers. These assumptions are in fact inappropriate for characterizing urban areas because our scatterers are buildings, walls, trees, etc., larger (and usually exceedingly larger) than the incident signal wavelength and certainly not tenuous.

As the *wave approach* seems to be inappropriate, a *ray approach* appears to be an attractive candidate, particularly in view of the large dimensions of the scatterers compared to the wavelength. In the related existing literature it is usually assumed that the communication channel can be represented by a *multipath* model [8]. Typically, the statistical characterization of the multipath component parameters has been performed by fitting data between some *suitable* probability distribution family and experimental measurements [9]–[13]. It is also certainly possible to conceive *ray launching* simulations for any given scenario, but this may pose a formidable *ray tracing* problem even for modern computers [14], [15]. Moreover, it is widely accepted that general conclusions and guidelines cannot be easily reached only on the basis of numerical simulations, even though there is no doubt that they usually constitute important validation of the theory.

The aim of this paper is to begin the exploration of an analytical solution to the above mentioned problem. We refer here to a very simplified canonical scenario as described in Fig. 1. The medium is composed of sites organized in a regular two-dimensional lattice. We consider here the simplest scenario of square sites, even though alternative choices are possible. (For instance triangular and honeycomb lattices are other possible two-dimensional structures, while cubic lattices and diamond

Manuscript received March 12, 1998; revised December 17, 1998.

G. Franceschetti is with the Dipartimento di Ingegneria Elettronica e delle Telecomunicazioni, Università degli Studi di Napoli "Federico II", Napoli, I-80125 Italy, and with the Department of Electrical Engineering, University of California, Los Angeles, California 90024-1594 USA.

S. Marano is with the Dipartimento di Ingegneria dell'Informazione ed Ingegneria Elettrica, Università degli Studi di Salerno, Fisciano (Salerno), I-84084 Italy.

F. Palmieri is with the Dipartimento di Ingegneria Elettronica e delle Telecomunicazioni, Università degli Studi di Napoli "Federico II", Napoli, I-80125 Italy, and with the Department of Electrical and Systems Engineering, University of Connecticut, Storrs, CT 06708 USA.

Publisher Item Identifier S 0018-926X(99)07064-7.

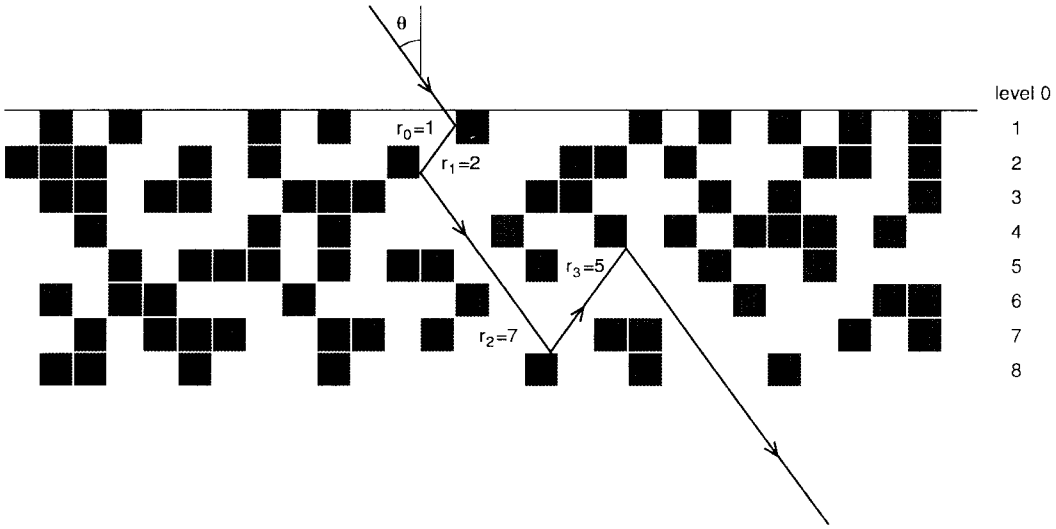

Fig. 1. Example of ray propagation in a square lattice.

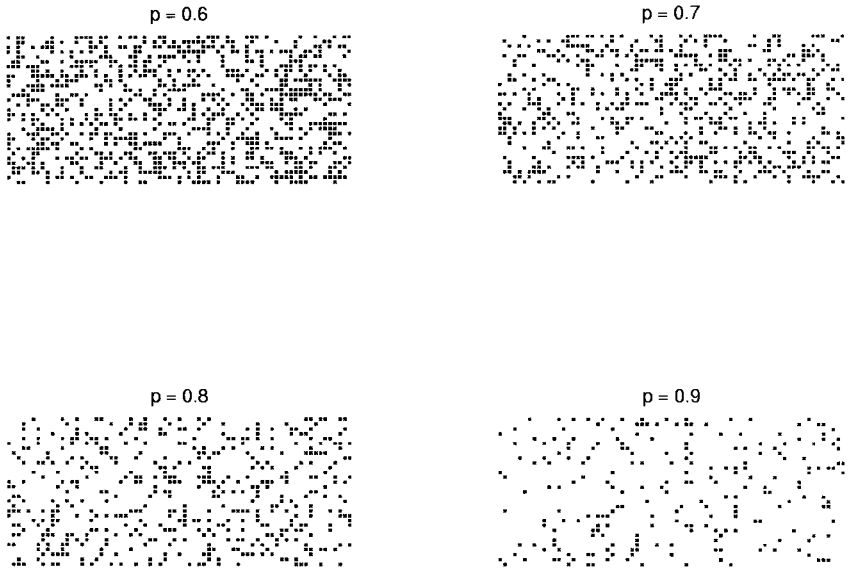

Fig. 2. Computer generated lattices with occupancy probability $q = 1 - p$.

lattices are examples of three-dimensional arrangements [16].) Each site can be either occupied, or empty. The arrangement is referred to as a *percolating lattice* and has been widely studied and used to model physical phenomena like forest fires, spin diffusions in ferromagnets, gelation of polymers, and other kinds of diffusion in random media [16].

Let us assume that the status (occupied or empty) of a cell is independent of the status of all other cells in the lattice (see next section) and assume that the occupancy probability is $q = 1 - p$. Given a very large lattice randomly occupied with probability q, percolation theory deals (among other topics) with the quantitative analysis of groups of neighboring empty sites (*clusters*): form, average size, number, etc. For modest values of p (say, p near zero) the average dimension of clusters is small, while for p near unity the lattice looks like a single cluster with sporadic holes. For p increasing from zero to one, there exists a certain critical value for which a large cluster of empty sites connecting the opposite sides of the lattice (top side and bottom side of the lattices in Fig. 2), appears for the first time. This critical value is named *percolating threshold* p_c and it has been estimated to be $p_c \approx 0.59275$ for the square geometry [16]. Near the percolating threshold the characteristics of the p-lattice change qualitatively, namely the structure exhibits a *phase transition*.

Our approach was originally inspired by the percolation theory, but it focuses on a rather different problem. In fact, we are interested in *ray propagation* instead of diffusion. Nevertheless, some aspects of the theory are of interest to us. For instance, a result of percolation theory that could turn out to be useful is the evaluation of the probability that two sites at a certain distance apart do not belong to the same cluster. The absence of a connection means that neither

diffusion nor ray propagation between the two sites is allowed. For this reason, in this work we limit our attention to the range of site occupancy such that the cell connection exists with sufficiently large probability, i.e., $p \in (p_c, 1)$. Therefore, we consider the medium for values of p already above the phase transition between *diffusion (propagation) prevented* and *diffusion (propagation) allowed*.

Consider now a monochromatic plane wave (in the Fig. 1 it is just a single ray) impinging at angle θ on a half-space filled by the scatterers. With reference to Fig. 1, we follow the path of a ray that undergoes successive reflections at levels $r_0, r_1, r_2, \cdots$, coincident with the rows of the lattice. We address (and answer) the following question. "What is the probability that the ray reaches (and eventually passes) the (row) level k?"

Other interesting questions are: "what is the probability that level k is reached at the Lth reflection?" and "what is the probability that R rays intercept at the same site in the lattice?" Answering to the former question is important when reflection losses needed to be included, while a solution for the latter question would allow a second-order statistical characterization of the transmitted field. We concentrate here on the propagation depth question leaving the other problems to a future study.

We understand that the scenario of Fig. 1 is an oversimplified version of the real propagation problem. In spite of this, its analytical solution constitutes to our knowledge a first rigorous result, totally new with respect to conventional propagation studies. Conclusions are by no means trivial and, we believe, of real practical importance. Determination of a *propagation depth* (as the answer to the stated question), which can be generalized up to the third dimension, may be relevant to estimation of the last mile actual size, giving a criterion for choosing electromagnetic compatible neighboring cell frequencies.

If the event that a site is empty or occupied is totally unrelated to neighboring site states, we have a completely random distribution of occupancies. Conversely, any statistical dependence among cells would mean that the scatterers are structurally organized. The limit case would be that of a fully ordered distribution of scatterers. Very structured lattices may be more appropriate models for modern cities that typically have a very regular distribution of buildings and streets. A (full) random model instead may fit better central parts of old towns (as common in Europe), when distribution of constructions proceeded with marginal rules over the years. In the following, we refer to this last model and assume that the generic site is occupied with probability q independently from all others sites.

This paper is organized as follows. In Section II, the model of the propagation channel is introduced and the lattice characteristics are briefly discussed. Sections III and IV deal with the statistical characterization of the random propagation process. In Section V, we first explore the exact numerical solution, and hence we derive analytical approximate formulas for the propagation depth. Section VI provides comparison between the derived formulas and numerical simulations. Final comments and conclusions are drawn in Section VII. The outline of the numerical procedure used to check the analytical approximations is deferred to Appendix A, while some analytical details are postponed to Appendix B.

II. The Propagation Model

Let us consider a regular lattice of square cells as depicted in Fig. 1. With no loss of generality, the side of such cells is assumed of unitary length. Each cell can be either occupied or empty. In the former case, an impinging ray is totally reflected according to the geometrical optics reflection laws; in the latter, the ray freely progresses. The scatterers are impenetrable so that the medium is lossless. Moreover, diffractions at the edges of the lattice are ignored. We assume further that the lattice has infinite horizontal extension; therefore, our results will be (statistically) invariant with respect to the horizontal coordinate. Also, the number of levels (in the vertical dimension) can be thought as infinite for our purposes. Four (computer generated) examples of (limited portion of) such percolating lattices, with values of $p = \{0.6, 0.7, 0.8, 0.9\}$ are depicted in Fig. 2.

The aim of our work is to answer the question stated in the previous section, for lattices characterized by a given value of p and for impinging waves with a prescribed incidence angle θ. Let us model the plane wave impinging on the lattice in terms of parallel rays and consider a ray entering the propagation medium with angle θ. The ray reaches the (row) levels $\{r_n, n \geq 0\}$ after successive reflections over the (occupied) sites (see Fig. 1). We have

$$r_n = r_0 + \sum_{m=1}^{n} x_m, \qquad n = 1, 2, \cdots \tag{3}$$

wherein r_0 is the initially reached level (at which the first reflection takes place) and the sequence

$$x_n = r_n - r_{n-1}, \qquad n = 1, 2, \cdots \tag{4}$$

is the level change after reflection n. For reasons that will be clear later, let us define also a *shifted version*, say $\{r'_n, n \geq 1\}$ of the sequence $\{r_n, n \geq 0\}$

$$r'_n = r_n - r_0 = \sum_{m=1}^{n} x_m, \qquad n = 1, 2, \cdots. \tag{5}$$

For a given lattice and prescribed incidence angle θ and entry position, the single ray path can be completely determined by the rules of geometrical optics. However, we are interested in the mean behavior of the propagation for a given value of the lattice density $1 - p$, hence, we associate to each randomly chosen lattice and ray entry point a different member function of the *stochastic process* $\{r_n, n \geq 0\}$. With this model we obtain a probabilistic characterization of $\{r_n, n \geq 0\}$ averaged over the ensemble of possible p-lattice realizations and possible entry points. In general, the random variables (RV's) x_n are statistically dependent and such a dependence is a function of the problem parameters. To make the problem tractable, however, we model x_n as independent RV's and, therefore, the sequence (3) has the structure of a classical random walk. We see in the following

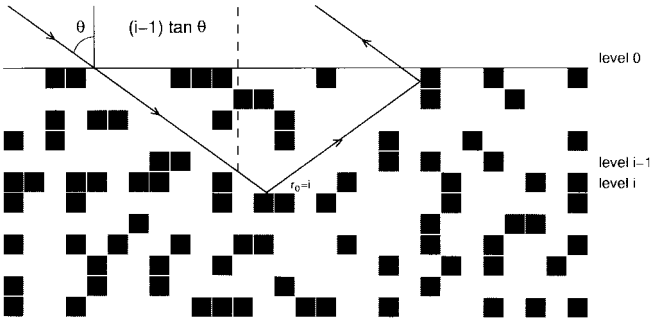

Fig. 3. Derivation of r_0's distribution.

that for certain values of the problem parameters p and θ this assumption is quite realistic, even though it may fail in other cases. These differences are highlighted in drawing comments on the simulation results.

Let us divide the problem at hand in two parts.

1) A half-space filled with scatterers is hit by a ray that undergoes a first reflection at level r_0. The first objective is to determine the statistics of r_0 (see Figs. 1 and 3).
2) Starting from level r_0, characterize the propagation of subsequent reflections. In other words, given r_0 for every depth $k \geq 0$, determine the probability that the ray intercepts that level before possibly escaping from level 0.

Following this framework in Sections III and IV, we derive the basic tools to deal with the abovementioned two issues.

III. Distribution of r_0

We derive hereafter the probability mass function (PMF) of r_0, $P_{r_0}(i) = \Pr\{r_0 = i\}$ with $i = 0, 1, 2, \cdots$. To this aim and with reference to Fig. 3, let us consider a ray entering the lattice with incidence angle θ. It is clear that the searched probability is equal to q for $i = 0$

$$P_{r_0}(0) = q. \tag{6}$$

For $i \geq 1$ such a probability can be computed as the product

$$\begin{aligned} P_{r_0}(i) = {} & \Pr\{\text{levels up to } i-1 \text{ are freely crossed}\} \\ & \times \Pr\{\text{a reflection takes place at level } i \textit{ given} \\ & \quad \text{that levels up to } i-1 \text{ are freely crossed}\}. \end{aligned}$$

The first factor equals p raised to the number of empty cells crossed by the ray to reach level i. This number equals the sum of crossed row and columns plus one (to have access at level i) that can be taken[1] to be $(i-1)(1+\tan\theta)+1$ (see Fig. 3). Accordingly

$$\begin{aligned} & \Pr\{\text{levels up to } i-1 \text{ are freely crossed}\} \\ & \quad = p^{(i-1)(1+\tan\theta)+1} = p_e^{i-1} p \end{aligned} \tag{7}$$

where

$$p_e = p^{1+\tan\theta} \quad \text{and} \quad q_e = 1 - p_e \tag{8}$$

are defined as *effective* probabilities of a site to be empty or occupied, respectively.

[1]The value should be bounded to an integer, but we ignore this fact.

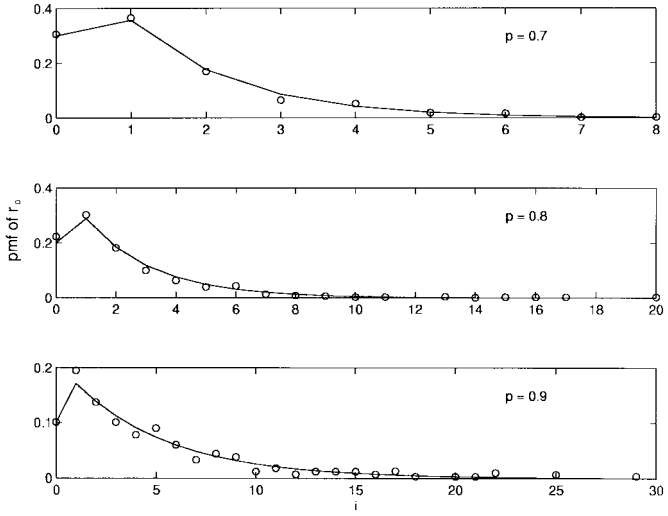

Fig. 4. Theoretical (line) and numerical (circles) values of $P_{r_0}(i)$ versus i, with $\theta^\circ = 45^\circ$.

A reflection at level i takes place if the first cell hit by the ray proceeding *into* the level i is occupied or if that cell is empty and the ray hits the next one, that must be occupied, and so on. Therefore, since the ray within the level i can cross at most $\tan\theta$ cells

$$\begin{aligned} & \Pr\{\text{a reflection takes place at level } i \text{ given that} \\ & \qquad \text{levels up to } i-1 \text{ are freely crossed}\} \\ & \quad = q \sum_{s=0}^{\tan\theta} p^s = q \frac{1 - p^{1+\tan\theta}}{1-p} = 1 - p_e. \end{aligned} \tag{9}$$

The final result is then

$$P_{r_0}(i) = \begin{cases} q, & i = 0, \\ p p_e^{i-1} q_e, & i > 0. \end{cases} \tag{10}$$

Note the role played by the effective probability of site occupancy $q_e \geq q$ that combines the effects of the incidence angle θ and of the probability of occupancy q. It is worth noting also that the random variable r_0 can be thought as the product of two independent RV's, say $r_0 = r_{01} r_{02}$. The former follows a geometric distribution with range $\{1, 2, \cdots, \infty\}$ and parameter q_e, i.e., $\Pr\{r_{01} = i\} = p_e^{i-1} q_e$ with $i = 1, 2, \cdots, \infty$. The latter is a Bernoulli RV with range $\{0, 1\}$ and parameter p, i.e., $\Pr\{r_{02} = 1\} = p$. The RV r_{02} models the discontinuity at the edge of the lattice (the ray enters the filled half piano with probability p), while r_{01} takes into account the propagation within the lattice, which is characterized by the effective probability of site occupancy q_e.

The analytical result of (10) has been validated by means of numerical experiments. Curves for different values of p and θ are depicted in Figs. 4 and 5, showing excellent agreement between simulation and theory. Details of the numerical procedure are postponed in Appendix A.

IV. Distribution of Successive Jumps

The characterization of the stochastic process involved in the study of the propagation depth requires computation of the PMF $P_{x_n}(i)$ of the (row) jump x_n. The analysis can be

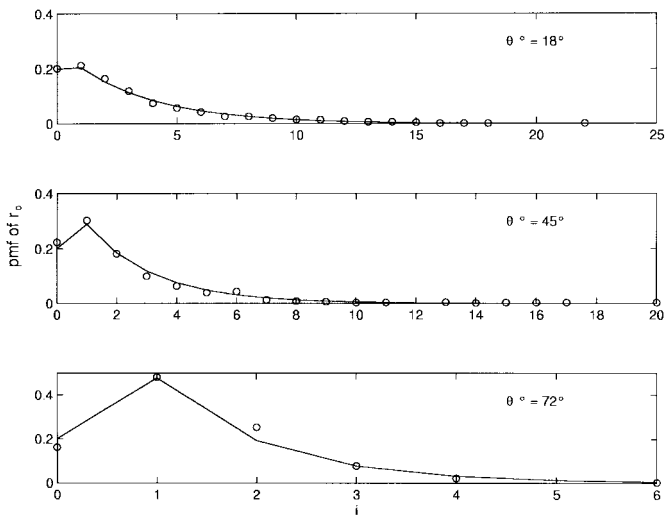

Fig. 5. Theoretical (line) and numerical (circles) values of $P_{r_0}(i)$ versus i, with $p = 0.8$.

developed by following the same lines of Section III and it is the topic of the present section.

With reference to Fig. 6, we can encounter three mutually exclusive situations.

1) There is no jump because the reflection takes place within the same (row) level i (in the figure it is the case of $r_2 = r_3 = 8$). This is easy to characterize by means of the same arguments yielding (9), giving $P_{x_n}(0) = q_e$.
2) There is a positive jump from level r_{n-1} to $r_n = r_{n-1} + i$ (in the figure for instance $r_5 = r_4 + 2$), that can be described by the following:

$$P_{x_n}(i) = \Pr\{x_n = i | x_n > 0\}\ \Pr\{x_n > 0\} = q_e p_e^{i-1}\ \Pr\{x_n > 0\} \tag{11}$$

where again $\Pr\{x_n = i | x_n > 0\}$ has been computed according to the same arguments used for $P_{r_0}(i)$ in Section III.
3) There is a negative jump from level r_{n-1} to level r_n (in the figure $r_2 = r_1 - 3$), giving

$$P_{x_n}(i) = q_e p_e^{|i|-1} \Pr\{x_n < 0\}. \tag{12}$$

Computation of the probabilities that the jump is positive or negative is now in order. We have

$$\Pr\{x_n > 0\} + \Pr\{x_n < 0\} = 1 - \Pr\{x_n = 0\} = 1 - q_e = p_e. \tag{13}$$

By supposing that the chances of both positive and negative jumps are on the same footing,

$$\Pr\{x_n > 0\} = \Pr\{x_n < 0\} = \frac{p_e}{2} \tag{14}$$

we get

$$P_{x_n}(i) = \tfrac{1}{2}\ q_e p_e^{|i|}, \qquad i \neq 0. \tag{15}$$

Unfortunately, a little thought shows that the above simple assumption may not always be true. In fact, examination of Fig. 6 clearly shows that a reflection on a horizontal face of a filled site inverts the sign of the jump, while the opposite effect holds for reflection on a vertical face. For an incidence angle θ we know that at every change in level, the ray hits $\tan\theta$ vertical barriers. Therefore, we can assume that the probability of hitting a vertical face is

$$\xi_v = \frac{\tan\theta}{1 + \tan\theta} \tag{16}$$

and that of hitting an horizontal face is

$$\xi_h = \frac{1}{1 + \tan\theta}. \tag{17}$$

Now $\Pr\{x_n > 0\}$ equals the probability of the event {out of n reflections, an even number of them has happened on horizontal faces *and* $x_n \neq 0$}. In

$$\Pr\{x_n > 0\} = \sum_{i=0}^{n}{}_{\text{even}} \binom{n}{i} \xi_h^i\, \xi_v^{n-i}\, p_e \tag{18}$$

$$= \frac{p_e}{2}\,[1 - (\xi_v - \xi_h)^n]. \tag{19}$$

In a similar way

$$\Pr\{x_n < 0\} = \frac{p_e}{2}\,[1 + (\xi_v - \xi_h)^n]. \tag{20}$$

Therefore, $\Pr\{x_n > 0\} = \alpha_n p_e$ and $\Pr\{x_n < 0\} = (1 - \alpha_n) p_e$, where

$$\alpha_n = \tfrac{1}{2} - \tfrac{1}{2}\,(\xi_v - \xi_h)^n. \tag{21}$$

In conclusion

$$P_{x_n}(i) = \begin{cases} q_e & i = 0 \\ \alpha_n\ q_e\ p_e^i & i > 0 \\ (1 - \alpha_n)\, q_e\, p_e^{|i|} & i < 0. \end{cases} \tag{22}$$

Note that we can think of x_n as the product of x_{n1}, a geometric RV with $\Pr\{x_{n1} = i\} = q_e p_e^i$ for $i = 0, 1, \cdots, \infty$ and x_{n2}, an RV of Bernoulli type for which $\Pr\{x_{n2} = 1\} = \alpha_n$ and $\Pr\{x_{n2} = -1\} = 1 - \alpha_n$. The latter takes into account the possibility of both positive and negative jumps, the former models the propagation into the lattice. Note also that $\lim_{n\to\infty}\ \alpha_n = 1/2$, namely the distribution tails tend to become symmetrical with a rate of convergence of α_n toward $1/2$ depending upon θ. We conclude that the distribution is only *asymptotically* symmetric zero-mean and the RV's x_n are only asymptotically identically distributed.

Also, in this case, analytical results have been tested by means of numerical experiments, as depicted in Figs. 7 and 8. The simulations average a sufficiently large number of realizations and can be considered to be asymptotic estimate with $\alpha_n = 1/2$. These results are detailed in Appendix A.

V. Evaluation of the Propagation Depth

In this section, evaluation of the propagation depth is carried out. First we explore the exact numerical solution to the propagation model under the assumption $r_n = r_0 + \Sigma_{m=1}^{n}\ x_m$ with independent and identically distributed (iid) x_n's. Unfortunately, the exact solution requires numerical manipulations of the transition matrix of the model, that do not appear to lend itself to a simple analytical expression. To

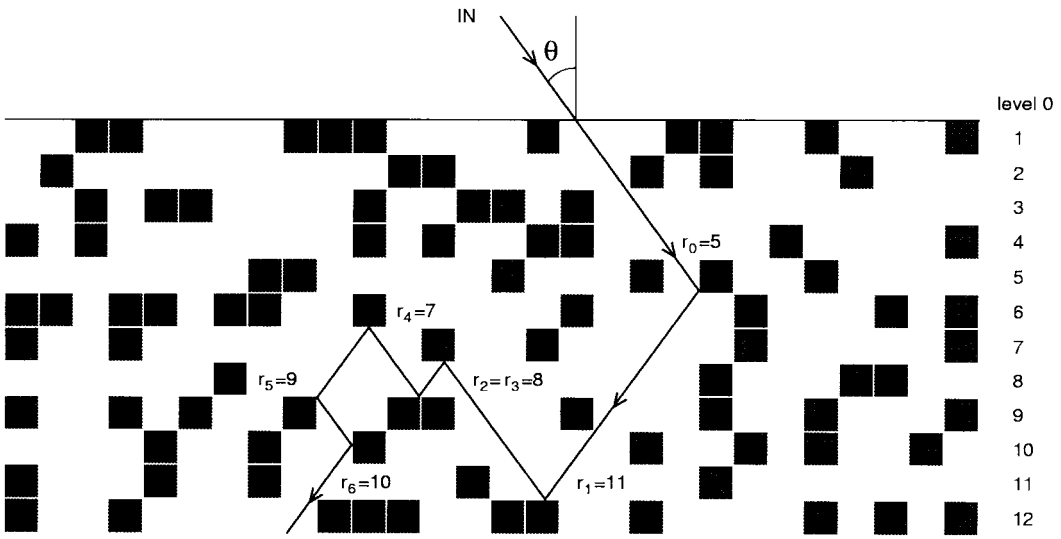

Fig. 6. Derivation of the x_n's distribution.

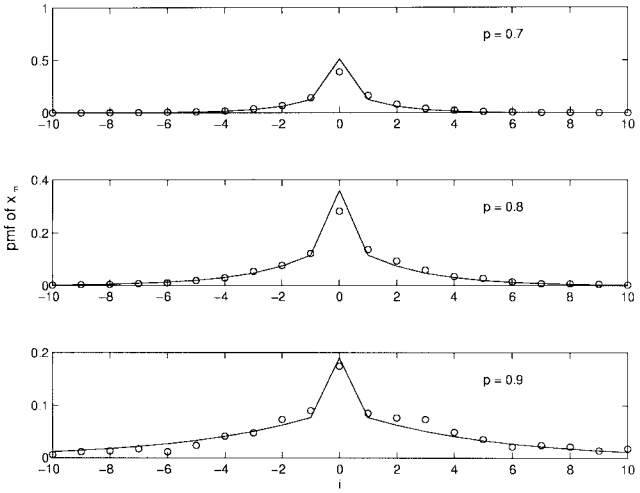

Fig. 7. Theoretical asymptotic (line) and numerical (circles) values of $P_{x_n}(i)$ versus i for $\theta^\circ = 45^\circ$.

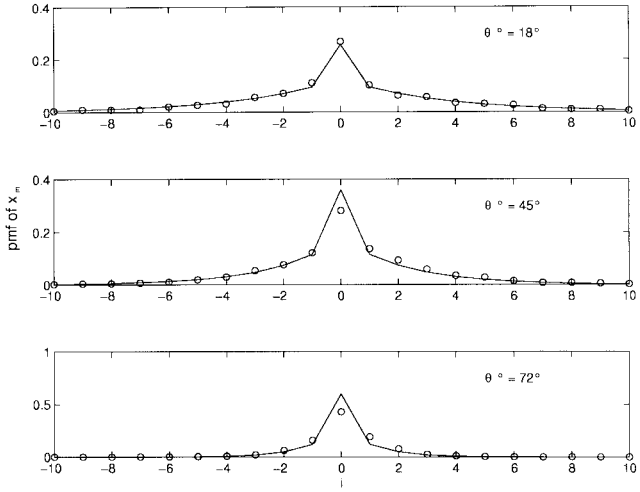

Fig. 8. Theoretical asymptotic (line) and numerical (circles) values of $P_{x_n}(i)$ versus i for $p = 0.8$.

more specifically understand the quantitative influence of the problem parameters p and θ on the propagation depth, we also develop an alternative approximate approach yielding a very simple analytical solution.

We would emphasize that both the exact and the approximate solutions refer to the assumed model. Numerical simulations confirm the adequacy of the model for most incidence angles θ and density parameters p.

A. Exact Solution

The propagation depth can be investigated on the basis of the classical Markov chain theory. In fact, the process of (3), within the assumption of independent jumps and with the asymptotic expression of the x_n's with $\alpha_n = 1/2\ \forall n$, obtained in the previous section, is an example of a homogeneous Markov chain. In particular, it is a random walk with two *absorbing* barriers (the interested reader is referred to [17]).

Let us think of the lattice levels $0, 1, 2, \cdots k$ as the possible *states* of a Markov chain. Consider state (level) zero as an absorbing state; when the rays hit such a level the process terminates and similarly for the state (level) k. Let us organize the probability of transition from state i to state j in a matrix M whose entries are

$$M(i,j) = \Pr\{r_n = j | r_{n-1} = i\}. \tag{23}$$

If we are away from the states zero and k, the transition probabilities are described by the jump (x_n's) distribution, i.e., $M(i,j) = P_{x_n}(|j-i|)$, $i,j = 1,2,\cdots,k-1$. Also, $M(0,0) = M(k,k) = 1$ and

$$M(i,0) = \sum_{j=-\infty}^{0} P_{x_n}(|j-i|) \qquad i = 1,2,\cdots,k-1,$$

$$M(i,k) = \sum_{j=k}^{+\infty} P_{x_n}(|j-i|) \qquad i = 1,2,\cdots,k-1$$

since the ray can overshoot over the barriers. The $(k+1)\times(k+1)$ transition matrix for the Markov chain is then seen in the equation at the bottom of the next page.

The initial state distribution of such a Markov chain is $P_{r_0}(i)$ for $i=0,1,2,\cdots,k-1$ and $\Sigma_{s=k}^{\infty}\,P_{r_0}(s)$ for $i=k$ that, organized in a vector (initial state distribution vector), gives

$$Q_0=\left[P_{r_0}(0),P_{r_0}(1),\cdots,P_{r_0}(k-1),\sum_{s=k}^{\infty}P_{r_0}(s)\right]^T. \quad (24)$$

If we denote with Q_n the state distribution vector at the $(n+1)$st reflection, we have

$$Q_n=\left[\sum_{s=-\infty}^{0}P_{r_n}(s),P_{r_n}(1),\cdots,P_{r_n}(k-1),\sum_{s=k}^{\infty}P_{r_n}(s)\right]^T.$$

(where $P_{r_n}(i)$ is the PMF of r_n) and obviously

$$\begin{aligned}Q_1^T&=Q_0^TM\\Q_2^T&=Q_0^TM^2\\&\vdots\quad\vdots\\Q_n^T&=Q_0^TM^n.\end{aligned} \quad (25)$$

The probability we are searching for is just the last entry of Q_n when n increases to infinity, i.e.,

$$\left(\lim_{n\to\infty}Q_n^T\right)_k=\left(Q_0^T\lim_{n\to\infty}M^n\right)_k. \quad (26)$$

The limit matrix $\lim_{n\to\infty}M^n$ can be evaluated (numerically) by spectral decomposition of M. It is obvious that the process, having two absorbing barriers, provides asymptotically a null vector Q_n except for the first and the last entries.

B. Approximate Analytical Solution

The solution provided above quite accurately reflects the propagation phenomenon. However, in this section, we also derive simple analytical (approximate) expressions that do not require the computation of the limit form of M^n. This gives us an easier-to-handle solution that also highlights more clearly the role of the problem parameters p and θ.

Let us start off again from the process (5) and fix a prescribed value of the RV $r_0, 0<r_0<k$. Compute the conditioned ensemble average

$$\begin{aligned}&\langle r'_{n+1}|x_n,x_{n-1},\cdots,x_1\rangle\\&\quad=\langle r'_n+x_{n+1}|x_n,x_{n-1},\cdots,x_1\rangle\\&\quad=\langle r'_n|x_n,x_{n-1},\cdots,x_1\rangle\\&\qquad+\langle x_{n+1}|x_n,x_{n-1},\cdots,x_1\rangle\\&\quad=r'_n+\langle x_{n+1}\rangle\end{aligned} \quad (27)$$

where the level jumps have been assumed statistically uncoupled from each other.

As $\langle x_n\rangle=0$, $\forall n$ i.e., positive and negative jumps are (asymptotically) equally likely (see Section IV) and $\langle|r'_n|\rangle<\infty$ (see Appendix B), the process $\{r'_n,n\geq 1\}$ can be considered a *martingale* with respect to $\{x_n,n\geq 1\}$ [18], [19], and

$$\langle r'_{n+1}|x_n,x_{n-1},\cdots,x_1\rangle=r'_n\qquad n=1,2,\cdots. \quad (28)$$

For a martingale, it is easily seen that $\langle r'_n\rangle=\langle r'_1\rangle$ for all n.

Consider now another random sequence, the *stopped process*, related to r'_n

$$\{\overline{r}'_n,n\geq 1\}=r'_1,r'_2,\cdots,r'_N,r'_N,r'_N,\cdots \quad (29)$$

wherein N is the smallest value between n_k and n_0 in Fig. 9; n_k is the number of jumps undergone by the ray to reach (and eventually pass) level k, whereas n_0 is the number of jumps to cross back to level zero and disappear. Formally, $N=\min\{n\text{: } r_n\geq k \text{ or } r_n\leq 0\}$. For instance, the ray on the left in Fig. 9 leaves the (effective) lattice after 21 reflections and $N=\min(n_0,n_k)=n_0=21$, while the ray on the right of the same figure reaches level k (and passes it hitting level $k+1$) after five reflections so that $N=\min(n_0,n_k)=n_k=5$. In the latter instance $r'_n=\overline{r}'_n$ for $n\leq 5$, whereas $r'_6=k, r'_7=k-1$ and $\overline{r}'_6=k+1, \overline{r}'_7=k+1$, etc. Within this formalism answering to the question stated in Section I means evaluating the probability $\Pr\{r_N\geq k\}$ or else $\Pr\{r'_N\geq k-r_0\}$ for a given value of r_0. In fact, this is the probability that the ray has reached at least depth k before escaping from the level zero.

It is useful to see the random walk $\{r'_n,n\geq 1\}$ as a martingale because a number of very general results are available in the literature and, in the following, we make explicit use of some of them. To this goal, we note that if $\{r'_n,n\geq 1\}$ is a martingale with respect to $\{x_n,n\geq 1\}$, then $\{\overline{r}'_n,n\geq 1\}$ is a martingale with respect to $\{x_n,n\geq 1\}$ [18] too and, consequently

$$\langle\overline{r}'_n\rangle=\langle\overline{r}'_1\rangle=\langle r'_1\rangle \quad (30)$$

$$M=\frac{1}{2}\begin{bmatrix}2&0&0&0&\cdots&0&0\\p_e&2q_e&q_ep_e&q_ep_e^2&\cdots&q_ep_e^{k-2}&p_e^{k-1}\\p_e^2&q_ep_e&2q_e&q_ep_e&\cdots&q_ep_e^{k-3}&p_e^{k-2}\\p_e^3&q_ep_e^2&q_ep_e&2q_e&\cdots&q_ep_e^{k-4}&p_e^{k-3}\\\vdots&\vdots&\vdots&\vdots&&\vdots&\vdots\\p_e^{k-1}&q_ep_e^{k-2}&q_ep_e^{k-3}&q_ep_e^{k-4}&\cdots&2q_e&p_e\\0&0&0&0&\cdots&0&2\end{bmatrix}$$

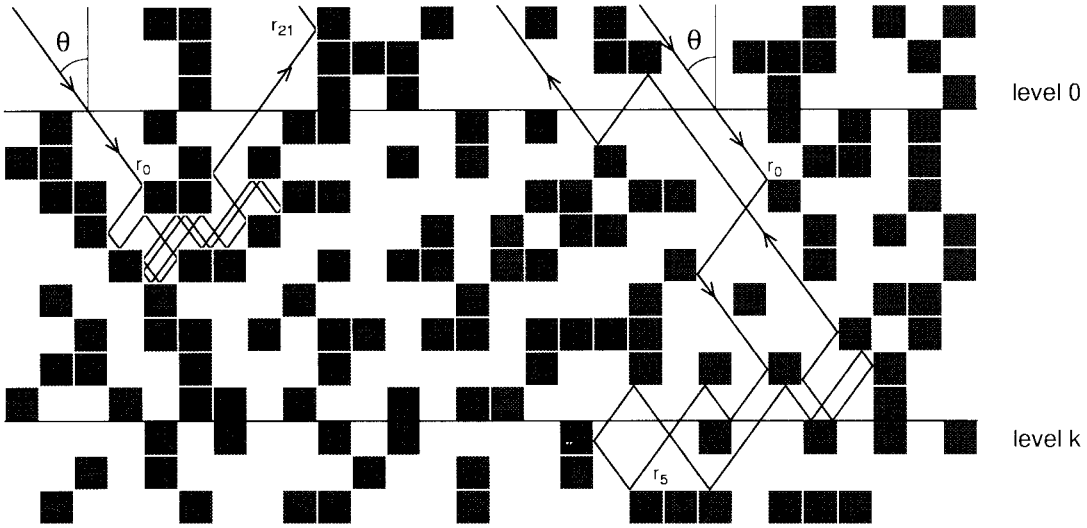

Fig. 9. Examples of propagating rays.

where the last equality derives from $\overline{r}'_1 = r'_1$. If $\Pr\{N < \infty\} = 1$, then for sufficiently large n, $\overline{r}'_n = r'_N$. This implies

$$\langle r'_1 \rangle = \lim_{n\to\infty} \langle \overline{r}'_n \rangle = \left\langle \lim_{n\to\infty} \overline{r}'_n \right\rangle = \langle r'_N \rangle \tag{31}$$

that finally yields

$$\langle r'_N \rangle = \langle x_1 \rangle = 0 \tag{32}$$

(for the assumption of zero mean x_n's). The interchange of limit and ensemble average in (31) is allowed by the martingale optional stopping theorem (see Appendix B for details).

Now

$$\begin{aligned} 0 = \langle r'_N \rangle = {} & \langle r'_N | r'_N \geq k - r_0 \rangle \ \Pr\{r'_N \geq k - r_0\} \\ & + \langle r'_N | r'_N \leq -r_0 \rangle \ \Pr\{r'_N \leq -r_0\} \end{aligned} \tag{33}$$

where $\Pr\{r'_N \leq -r_0\} = 1 - \Pr\{r'_N \geq k - r_0\}$.

A first approximation (usually referred to as Wald's approximation) is to assume

$$\langle r'_N | r'_N \geq k - r_0 \rangle \approx k - r_0 \tag{34}$$

$$\langle r'_N | r'_N \leq -r_0 \rangle \approx -r_0. \tag{35}$$

The first equation basically means that when the ray overcrosses the level $k - r_0$, it does not overcross it significantly. A similar interpretation holds for the second relationship. With these assumptions, (33) yields

$$\Pr\{r'_N \geq k - r_0\} \approx r_0/k. \tag{36}$$

Actually, the previous probability is conditioned on r_0, (namely represents $\Pr\{r_N \geq k | r_0\}$) and, until now, we have considered the case of $0 < r_0 < k$. In the general case, a little thought should convince us that

$$\Pr\{r_N \geq k | r_0 = i\} \approx \begin{cases} 0, & i = 0 \\ i/k, & 0 < i < k \\ 1, & i \geq k. \end{cases} \tag{37}$$

To release the conditioning over r_0, ensemble expectation of last relationship with respect to distribution (10) has to be performed. This yields (after some algebra)

$$\Pr\{r_N \geq k\} \approx \frac{p}{q_e\, k} \left(1 - p_e^k\right) \tag{38}$$

that is, the searched results. It is important to stress that the distribution of x_n does not play a role in deriving relationship (38) (except for verifying regularity conditions for validity of (32)—see Appendix B); all that is required is the zero-mean property of the x_n's. As a check for (38), note that

$$\lim_{p\to 0} \frac{p}{q_e\, k} \left(1 - p_e^k\right) = 0$$

$$\lim_{p\to 1} \frac{p}{q_e\, k} \left(1 - p_e^k\right) = 1$$

as expected.

An improvement of the approximation of (38) can be derived by exploiting the distribution (22) of the x_n's. In fact

$$\begin{aligned} \langle r'_N | r'_N \geq k - r_0 \rangle &= \langle r'_{N-1} | r'_N \geq k - r_0 \rangle \\ &\quad + \langle x_N | r'_N \geq k - r_0 \rangle \\ &\approx 0 + \langle x_N | x_N \geq k - r_0 \rangle \\ &= k - r_0 + \frac{p_e}{q_e}. \end{aligned} \tag{39}$$

The approximation consists in substituting everywhere in the right-hand side of the first equality of the previous expression r'_{N-1} with its expectation zero. Then the evaluation of $\langle x_N | x_N \geq k - r_0 \rangle$ is performed basing upon the distribution of the x_n's (note that the previous approximation, lacking of knowledge of the statistical characterization of x_n's, was to assume further $\langle x_N | x_N \geq k - r_0 \rangle \approx k - r_0$). In a similar fashion

$$\langle r'_N | r'_N \leq -r_0 \rangle \approx -r_0 - \frac{p_e}{q_e}. \tag{40}$$

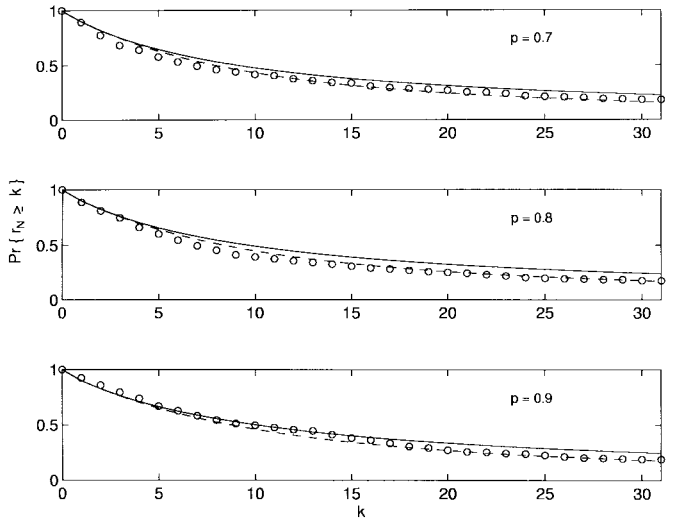

Fig. 10. Probability that the propagation depth is greater than k versus k for different values of p and for $\theta^\circ = 45^\circ$. The dashed line represents Wald's approximation of (38). The solid line represents the exact solution obtained by (26) using spectral decomposition of the matrix M and also (42). Circles denotes simulated values.

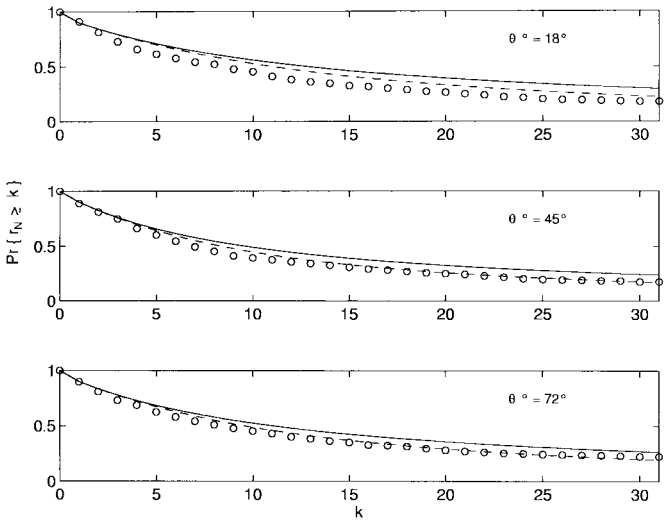

Fig. 11. Probability that the propagation depth is greater than k versus k for different values of θ and for $p = 0.8$. The dashed line represents Wald's approximation of (38). The solid line represents the exact solution obtained by (26), practically indistinguishable from the values obtained from (42). Circles denotes simulated points.

This yields

$$\Pr\{r_N \geq k | r_0 = i\} = \begin{cases} 0, & i = 0 \\ \dfrac{i + p_e/q_e}{k + 2p_e/q_e}, & 0 < i < k \\ 1, & i \geq k. \end{cases} \quad (41)$$

After expectation with respect to r_0, we get

$$\Pr\{r_N \geq k\} \approx \frac{p}{q_e} \frac{1 + p_e}{k + 2p_e/q_e}. \quad (42)$$

Within this improvement, the density of the lattice and the angle of the ray are taken into account when the ray is supposed to overcross the level k or the level zero (see Fig. 9). Note also that to the limits $p \to 0/1$ (42) behaves like (38). It is remarkable that from a numerical point of view, relationship (42) is practically coincident for all values of p and θ of interest, with the exact solution outlined in Section V-A (see next section). Hence, it can be considered as the right (nonapproximate) expression of the propagation depth. The obvious advantage over the exact solution drawn before relies in the simple and analytical form of (42).

VI. Numerical Simulations

The final results summarized in (38) and (42) have been verified by extensive simulations. Figs. 10 and 11 report the comparison of a computer-based ray launching experiment and the analytical results for a few values of p and θ. The circles represent the experimental points whereas the dashed line and the solid line correspond to (38) and (42), respectively. The last curve is practically indistinguishable from the one obtained with (26) using the (numerical) spectral representation of matrix M.

The three plots of Fig. 10 refer to different values of p, while the angle of incidence has been chosen $\theta^\circ = 45^\circ$. The matching between the simulated data and the analytical approximations is quite good for values of $p \in (0.7, 0.9)$. Naturally, the analytical approximation is not applicable for values of p too close to unity or values which are too small, i.e., near percolation threshold $p_c = 0.592\,75$. In fact, in a sparse medium the propagation looks like propagation in free-space and the reflections are events with probability close to zero. Conversely, in a dense medium the large probability of *loops* (repeated reflections over the same few cells) suggests that the propagation is practically inhibited, and the assumption of statistically uncoupled jumps would loose validity. It should be noted that these extreme cases are of limited practical interest for the communication problem at hand.

In Fig. 11 we fix $p = 0.8$ and compare the analytical formulas with the simulations by varying θ. Once again the exact solution [see (26) in Section V-A] is practically indistinguishable from approximation (42). It turns out also that the matching with experimental values is excellent when $\theta^\circ \approx 45^\circ$, whereas the approximation is less accurate for values of θ close to zero or 90°. This is not surprising because for values of θ far from 45° the hypothesis of independence between the x_n's is questionable. Note, in fact, that when $\theta \to 90^\circ$ there is a large probability of reflections between the *same* two cells at the same level so that with high probability $x_n = x_{n+1} = 0$ for several values of n. Analogously, for values of θ too close to zero with high probability, there is just a single reflection, i.e., the x_n's are not defined at all and the random process *collapses* in the single variable r_0 following distribution (10) with $\theta \approx 0$.

As an example of a situation in which the proposed approach is not applicable we consider just the limit case of $\theta = 0$. Fig. 12 clearly shows that the probability of propagation depth closely follows the formula (in the figure it is represented by the dash-and-dot line)

$$\Pr\{r_N \geq k\} = p^k, \qquad k = 0, 1, 2, \cdots. \quad (43)$$

This is the complement of the cumulative distribution of r_0, with $\theta = 0$. Note that neither Wald's approximation (solid

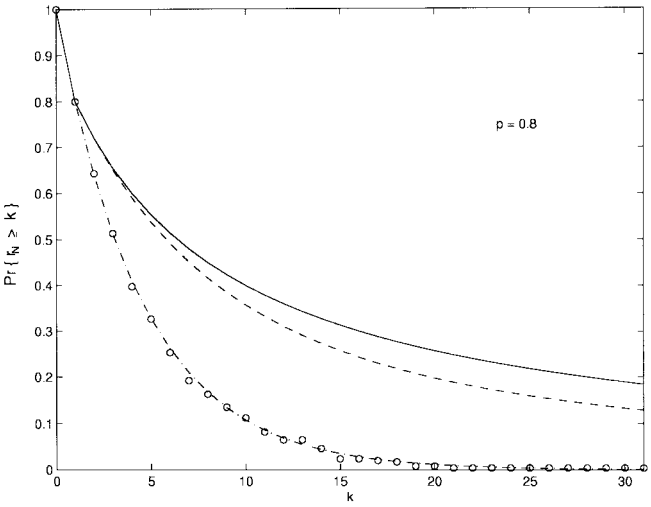

Fig. 12. Probability that the propagation depth is greater than k versus k for $p = 0.8$ and $\theta^{\circ} = 0^{\circ}$. The dashed line represents Wald's approximation. The solid line obeys (26), and it is practically indistinguishable from the values obtained from (42). Circles denotes simulated values and dash-and-dot line describes formula (43).

line) nor the alternative (exact) formula (42) (dashed line) are able to describe with sufficient accuracy the simulated values (circles).

VII. Conclusions

Propagation in random media is a suitable model for a large class of communication problems, including the last mile issue and the characterization of urban area radio channels. The aim of this paper has been to begin an analytical investigation of such a topic by considering a simple scenario in which a plane wave approaches a half space of random scatterers.

The plane wave is modeled as an ensemble of parallel optical rays with a given incidence angle θ. The half-space is modeled as a regular lattice of square sites and it is characterized by the probability q that a given site is occupied by a scatterer. The propagation of the rays in the lattice is assumed to obey the rules of the geometrical optics: when the ray hits a scatterer it is completely reflected. Conversely, the propagation behaves as in free-space when empty sites are hit. To make the problem tractable we further assume that the ray propagation can be modeled as a random walk process in which the ray jump after nth reflection over an occupied site is independent of all previous jumps.

We have focused on evaluating the probability that a ray reaches a given level in the half-plane, which represents the capability of the wave to penetrate into the medium.

We have introduced an effective site occupancy probability $q_e = 1-(1-q)^{1+\tan\theta}$ that summarizes the effects of the incidence angle θ and of the probability of occupancy q on the ray propagation mechanism. Then, the statistical characterization of the propagation process was carried out based on combining geometrical considerations with probability theory concepts.

Using these results, we have shown that an exact solution for the probability of reaching a given level in the half plane can be obtained by exploiting the theory of Markov chains, which unfortunately requires numerical methods for the computation of the limit form of the transition matrix.

Therefore, we have been encouraged to proceed toward an analytical approximate solution in which the roles of the density of the lattice q and of the plane wave incidence angle θ are well highlighted. This goal has been achieved making use of the powerful tool of the martingale theory, resulting in two different approximations.

Both the derived exact solution and the analytical approximate formulas have been tested by means of simulations. This analysis validates the adopted model for a wide range of values of q and θ. However, for values of q that correspond to very dense or very sparse lattices and for incidence angles θ close to normal or radent, the model looses accuracy. These cases must be handled by a different approach which is a topic of current investigation.

Extensions of the theory under investigation include the case of a whole plane filled by random scatterers with an internal and isotropic ray source and the loss evaluation (number of reflections) when the ray reaches a given level.

Appendix A
Outline of the Numerical Procedure

This section is devoted to describing the numerical procedure, realized in MATLAB, designed to check the analytical results obtained above. Basically, the numerical method consists of generating a (large) number of random lattices. In each lattice a (large) number of rays are *launched* and their propagation is asked to obey the simple rules of geometrical optics. Being each sequence of reflection levels a realization of the random process $\{r_n, n \geq 1\}$, the statistical properties of such a process can be estimated from this collection of data.

More precisely, we consider a square matrix of $h \times h$ elements, with one and zero entries. Each entry is a realization of a Bernouilli RV assuming value one with probability q. Therefore, the symbol "1" corresponds to the occupied cells and the "0" to the empty ones. The status of each cell is independent of that of all the other cells.

Each cell is labeled by row and column indexes (i, j) and supports its own coordinate system. A first coordinate, say l, denotes one of the four sides—north, east, south, and west. One each side an abscissa $a \in (0, 1)$ is defined (the square cell is assumed to have unitary length), having the origin behind an observer proceedings in clockwise direction on the cell frontier. Finally, the angle ϕ that the direction of the ray propagation forms with respect to the outstanding versor of the considered side l represents the last coordinate. The angle $\phi \in (-\pi/2, \pi/2)$ is assumed to be positive if the direction of propagation lies in the quadrant delimited by the side at hand, the outstanding versor, and containing the origin of the abscissa (the point $a = 0$); otherwise, ϕ is negative.

Within this formalism is very simple to simulate the ray propagation in the lattice. Let us assume that a ray at the generic program step s is leaving the cell (i_s^o, j_s^o) in the position defined by (l_s^o, a_s^o, ϕ_s^o). The corresponding coordinate vector will be $\Omega_s^o = [i_s^o, j_s^o, l_s^o, a_s^o, \phi_s^o]$ (^{o} means output coordinate). Then, the simulation program checks for the status of

the cell that the ray is trying to enter. If it is occupied, the cell crossed by the ray remains the same ($i_s^i = i_s^o, j_s^i = j_s^o$), and new input coordinates ($l_s^i = l_s^o, a_s^i = a_s^o, \phi_s^i = -\phi_s^o$) (^{i} stems for input) are computed. These define the vector Ω_s^i. The level position of the reflection (i.e., the current value of the row index i) is memorized for subsequent statistical analysis. Conversely, if the cell is not occupied the propagation proceeds to a new site. Also, in this case, it is straightforward to write the input vector Ω_s^i. Finally, the program evaluates the exit point of the ray from the cell at hand (by simple geometric rules), obtaining a new Ω_{s+1}^o. Hence, the single program step is completed.

To initialize the algorithm the ray is supposed to approach the lattice from above $i = 1$, $l =$ north, with random column index $j = 1, 2, \cdots, h$ and random abscissa $a \in [0, 1)$. The angle ϕ being determined by the plane wave incidence angle θ. The simulation stops when the ray is either approaching level zero (top of the lattice) or approaching level $h + 1$ (lattice bottom side).

For rays approaching the lateral sides of the lattice (namely, if a ray tries to enter cells with either $j^i = 0$ or $j^i = h + 1$ column index) the simulation program provides to reinject such rays (with the proper coordinates) from the opposite side of the lattice. In this way, the number of columns in the lattice is virtually infinite or, otherwise stated, the structure is *periodic* in the horizontal direction. This does not seem to represent a serious drawback on the basis of the following reasoning. Let us consider the functional relationship between the entry point of a ray $(j_{\text{in}}, a_{\text{in}})$ in the lattice and its exit point from a lateral side $(i_{\text{out}}, j_{\text{out}}, a_{\text{out}})$ (but the same holds true more in general): $(j_{\text{in}}, a_{\text{in}}) = f(i_{\text{out}}, j_{\text{out}}, a_{\text{out}})$. A simulation evidence is that a slight variation in the input coordinates can correspond to completely different output coordinates. In this sense, the function $f(\cdot)$ appears to be *chaotic* because, even though $f(\cdot)$ represents a deterministic rule, the lateral exit point corresponding to a *given* entry point can be thought as *random*. Hence, the entry point on the opposite lateral side computed by the program is a random function of the input. But *random* lateral entry points behave like fixed lateral entry points for rays propagating in different lattice realizations. Therefore, even though the structure is periodic, its equivalent behaviors is essentially that of a single p lattice with infinite horizontal dimension.

To ensure statistical significance, the simulation program generates a certain number of rays in the same lattice to "catch" the mean behavior of the propagation (the sequence of reflection levels, for our purposes) with respect to the ray enter position. Results reported in this paper refers to 500 rays per lattice. Then, the whole process is repeated for different lattices (with the same p and the same θ). We found that a number of lattices in the order of $50 \div 100$ allows for suitable statistical investigation and it is compatible with the simulation time constraints.

With the described procedure we collect the sequences of reflection levels and evaluate the probabilistic quantities under investigation. Precisely, with reference to Figs. 4 and 5 we are interested in estimating the PMF of r_0. Then, we consider only the first sample of each simulated sequence and compute the number of realizations equals k divided by the total number of generated sequences. This ratio is the searched $P_{r_0}(\cdot)$ estimate.

Let us focus on Figs. 7 and 8. There, the experimental values of the x_n's PMF have been evaluated assuming identically distributed RV's. That is to say, the values x_n for different n have been considered as realizations of the *same* random variable, and Figs. 7 and 8 report the empirical PMF of such a variable. We have shown that this is allowed only in the asymptotic case of $\alpha_n = 1/2$. For this reason, such a simulation does not allows for testing the validity of (22). However, further deeper investigations on the distribution of the single $x_1, x_2, \cdots$ (for brevity not detailed here), seem to confirm that the asymptotic behavior is usually achieved after a few reflections. Such experiments seem to justify the adoption of a distribution with symmetric tails with $\alpha_n = 1/2$.

Finally, the experimental values of the propagation depth, as depicted in Figs. 10 and 11, have been obtained by simply evaluating the fraction of realizations for which at least one sample exceeds the given value of k.

APPENDIX B
REGULARITY CONDITIONS FOR THE MARTINGALE r'_n

In this section, the formal justification of interchange of limit and ensemble average in (31) is provided. First let us introduce the concept of *random time*. The integer values (possibly infinity) RV N is called *random time* (also Markov time) for the process $\{x_n, n \geq 1\}$ if the event $\{N = n\}$ is determined by the RV's $x_1, x_2, \cdots x_n$. In other words N is a random time for $\{x_n,\ n \geq 1\}$ if we can decide if $\{N = n\}$ or not from knowledge of values x_i from $i = 1$ up to $i = n$. Moreover, if $\Pr\{N < \infty\} = 1$ then the random time is called *stopping time*. The RV N introduced in (29) is in fact a random time.

We use now the following result [18, Th.7.2.2, p. 231], [19, Cor. 3.1., p. 260] known as *martingale optional stopping theorem*. Let $\{r'_n, n \geq 1\}$ be a martingale and N a random time with respect to $\{x_n,\ n \geq 1\}$. If

$$\langle N \rangle < \infty \tag{44}$$

and there exists a constant $K < \infty$ such that

$$\langle |r'_{n+1} - r'_n| | x_n, x_{n-1}, \cdots, x_1 \rangle \leq K, \qquad \text{for } n < N \tag{45}$$

then

$$\langle r'_N \rangle = \langle r'_1 \rangle. \tag{46}$$

By means of such a result we have only to show conditions (44) and (45) to hold for the martingale at hand. We verify that this is the case for (22) with $\alpha_n = 1/2$ (namely, asymptotic PMF of the jumps).

Let us start with $\langle N \rangle < \infty$. Assume that $\Pr\{x_n = 0\} \neq 1$ (nondegenerate RV), then $\exists$ an integer T and $0 < \delta < 1$ such that $\Pr\{|r'_T| > k\} > \delta$. Introducing the auxiliary RV's $Y_1 = r'_T, Y_2 = r'_{2T} - r'_T, \cdots, Y_i = r'_{iT} - r'_{(i-1)T}$ it results that

$$\Pr\{N \geq iT\} \leq \Pr\{|Y_1| \leq k\} \cdots \Pr\{|Y_i| \leq k\} \leq (1 - \delta)^i$$

and, hence,

$$\langle N\rangle = \sum_{i=1}^{\infty} \Pr\{N \geq i\} \leq T \sum_{i=0}^{\infty} \Pr\{N \geq iT\}$$
$$\leq T \sum_{i=0}^{\infty} (1-\delta)^i = \frac{T}{\delta} < \infty.$$

Note also that a similar reasoning leads to the conclusion that $\Pr\{N < \infty\} = 1$, i.e., the random time is actually a stopping time.

For what concerns relation (45), noting that $|x_n|$ is simply a geometric RV of parameter q_e (and, hence, with expectation p_e/q_e), we immediately get

$$\langle |r'_{n+1} - r'_n| | x_n, \cdots, x_1\rangle = \langle |x_{n+1}| | x_n, \cdots, x_1\rangle$$
$$= \langle |x_{n+1}|\rangle = \frac{p_e}{q_e}$$

which ends the proof.

Before concluding this section, we check for condition $\langle |r'_n|\rangle < \infty$ needed to ensure the martingale property of $\{r'_n\}$

$$\langle |r'_n|\rangle \leq \sum_{i=1}^{n} \langle |x_i|\rangle = n\frac{p_e}{q_e} < \infty$$

being $q_e \geq q$ and assuming $q > 0$ (to avoid trivialities).

REFERENCES

[1] C. C. Yu, D. Morton, C. Stumpf, R. G. White, J. E. Wilkes, and M. Ulema, "Low-tier wireless local loop radio systems—Part 1: Introduction," and "—Part 2: Comparison of systems," *IEEE Commun. Mag.*, vol. 35, pp 84–98, Mar. 1997.

[2] "La Radio per l' Ultimo Miglio (Sistemi Terrestri)," Interim Rep., Ver. no. 2, CSELT, Italy, June 13 1997 (in Italian).

[3] L. Bernstein, C. M. Yuas, "Managing the last mile," *IEEE Commun. Mag.*, vol. 35, pp. 72–76, Oct. 1997.

[4] S. Dehghan and R. Steel, "Small cell city," *IEEE Commun. Mag.*, vol. 35, pp. 52–59, Aug. 1997.

[5] A. Ishimaru, *Wave Propagation and Scattering in Random Media*. San Diego, CA: Academic,, 1978, vols. 1, 2.

[6] M. Kerker, *The Scattering of Light*. New York: Academic, 1969.

[7] B. J. Berne and R. Pecora, *Dynamic Light Scattering*. New York: Wiley, 1976.

[8] J. G. Proakis, *Digital Communications*, 3rd ed. New York: McGraw-Hill, 1995.

[9] G. Turin, F. D. Clapp, T. L. Johnston, S. B. Fine, and D. Lavry, "A statistical model of urban multipath propagation," *IEEE Trans. Veh. Technol.*, vol. VT-21, pp. 1–9, Feb. 1972.

[10] H. Suzuki, "A statistical model of urban radio propagation," *IEEE Trans. Commun.*, vol. 25, pp. 673–680, July 1977.

[11] H. Hashemi, "Impulse response modeling of indoor radio propagation channels," *IEEE J. Select. Areas Commun.*, vol. 11, pp. 967–978, Sept. 1993.

[12] L. Talbi and G. Y. Delisle "Experimental characterization of EHF multipath indoor radio channels" *IEEE J. Select. Areas Commun.*, vol. 14, pp. 431–439, Apr. 1996.

[13] L. Dossi, G. Tartara, and F. Tallone, "Statistical analysis of measured impulse response functions of 2.0-GHz indoor radio channels," *IEEE J. Select. Areas Commun.*, vol. 14, pp. 405–410, Apr. 1996.

[14] E. Damosso and F. Tallone, "Coperture radio per ambienti microcellulari urbani: il caso DECT," *Notiziario Tecnico Telecom Italia*, year 6, no. 1, pp. 67–78, July 1997 (in Italian).

[15] G. E. Corazza, V. D. Esposito, M. Frullone, and G. Riva, "A characterization of indoor space and frequency diversity by ray-tracing modeling," *IEEE J. Selected Areas Commun.*, vol. 14, pp. 411–419, Apr. 1996.

[16] D. Stauffer, *Introduction to Percolation Theory*. London, U.K.: Taylor Francis, 1985.

[17] W. Feller, *An Introduction to Probability Theory and Its Applications*. New York: Wiley, 1966, vol. II.

[18] R. M. Ross, *Stochastic Processes*. New York: Wiley, 1983.

[19] R. Karlin and H. M. Taylor, *A First Course in Stochastic Processes*, 2nd ed. San Diego, CA: Academic, 1975.

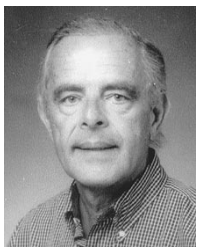

Giorgio Franceschetti (S'60–M'62–SM'85–F'88) was appointed Full Professor of Electromagnetic Wave Theory at University of Naples, Italy. He has been Visiting Professor at the University of Illinois (1976 and 1977), University of California at Los Angeles (UCLA) (1980 and 1982), National Somali University (1984), Somalia, and the University of Santiago de Compostela (1995), Spain. He was a Research Associate (1981 and 1983) at California Institute of Technology, Pasadena, CA. He has lectured in several summer schools in China, Great Britain, Holland Italy, Spain, Sweden, and the United States. He has published approximately 120 journal papers in the field of applied electromagnetics and synthetic aperture radar (SAR). He is an Adjunct Professor at UCLA, and a Distinguished Visiting Scientist at the Jet Propulsion Laboratory, Pasadena, CA

Prof. Franceschetti was Director of IRECE, a Research Institute of the Italian National Council of Research (CNR) and a former member of the Board of Directors of the Italian Space Agency (ASI). He was a Fulbright Scholar in 1973.

Stefano Marano received the "Laurea" in electronic engineering from the University of Naples, Italy, in 1993, and the Ph.D. degree in electrical engineering and computer sciences, from the same university, in 1997.

From 1997 to 1999, he has held teaching and research position at both the University of Naples and the University of Salerno, Italy. In February 1999 he joined the Department of Information Engineering and Electrical Engineering, University of Salerno, where he received a post Ph.D. Fellowship. His research interests are in the areas of statistical signal processing, with an emphasis on detection and estimation, electrical communications, and information theory.

Francesco Palmieri received the "Laurea" degree in electronic engineering (*cum laude*) from Universita' degli Studi di Napoli "Federico II," Italy, in 1980, and the M.S. (applied sciences) and Ph.D. degrees (electrical engineering) from University of Delaware, Newark, in 1985 and 1987, respectively.

In 1981, he served as a second Lieutenant in the Italian Army in fullfillment of draft duties. In 1982 and 1983 he was with ITT, FACE SUD Selettronica in Salerno, Italy, and Bell Telephone Manufacturing Company, Antwerpen, Belgium, as a Designer of digital telephone systems. He was appointed Assistant Professor in Electrical and Systems Engineering, University of Connecticut, Storrs, in 1987, where he was awarded tenure and promotion to Associate Professor in 1993. He is presently with the Department of Electronics, Universita' degli Studi di Napoli "Federico II," Italy, where he is an Associate Professor of electrical communications. His research interests are in the areas of signal processing, electrical communications, information theory, and neural networks.

Dr. Palmieri was awarded a Fulbright Scholarship in 1983 from the University of Delaware.